

Millimeter Wave Molecular Beam Spectroscopy: Alkali Bromides and Iodides*

JAMES R. RUSK AND WALTER GORDY

Department of Physics, Duke University, Durham, North Carolina

(Received March 22, 1962)

The pure rotational spectra of the alkali bromides and the alkali iodides were investigated in the 1.5 to 5.0 mm range of the microwave region. The experiment was performed by passing a beam of molecules in the vapor state from an oven, capable of producing temperatures up to 1000°C, into an oversized section of wave guide so that the direction of incident microwave radiation was at right angles to the flow direction of the molecular beam. In this way linewidths less than 100 kc/sec at 100 000 Mc/sec were easily achieved. The line frequencies were measured with a precision better than one part in 10^6 . The apparatus was developed as a series of modifications on an earlier experiment performed at this laboratory. Dunham's theory for diatomic molecules was applied in interpretation of the data. In most cases, the values for B_e , α_e , and γ_e were known although less accurately, but D_e and β_e were found for the first time. From the latter two, accurate determinations were made for the first time of ω_e and $\omega_e x_e$. From these values, information has been obtained about the potential functions, which suitably describe these diatomic alkali halides. In addition, centrifugal distortion constants, isotope mass ratios, moments of inertia, and internuclear distances have been accurately evaluated for each molecule.

INTRODUCTION

EARLIER it was demonstrated in this laboratory that rotational absorption spectra of collimated molecular beams at high temperature can be directly detected in the millimeter wave region by observation of the dip in the detected power as the frequency of the radiation source is swept through the spectral frequency.¹ We have improved this method and have used it to measure precisely millimeter wave transitions for most of the alkali halides.

Our molecular beam spectrometer complements rather than overlaps the applicability of the earlier molecular beam resonance methods^{2,3} which employ molecular rather than radiation detectors. The electric resonance method² is applicable principally at radio frequencies or in the long-wave microwave region where the molecules are sensitive to Stark fields, whereas the present, direct-absorption method is principally applicable at the high millimeter or submillimeter wave frequencies, where the absorption coefficients of molecules become large. As is seen from the results in this paper, complete and accurate solution for the spectral constants of diatomic molecules requires measurements at a number of frequencies, including those in the millimeter wave range.

Rotational absorption spectra of many alkali halides have been measured earlier by Honig, Mandel, Stitch, and Townes^{4,5} in the centimeter wave range with a conventional microwave spectrometer having a specially designed absorption cell which could be heated to the

high temperatures necessary for vaporization of these molecules. Their method is similar to ours in that it employs a radiation detector rather than the more specialized molecular detector of the electric and magnetic resonance methods. It differs from ours in that it does not employ molecular beams to avoid, or reduce, the considerable Doppler broadening and collision broadening encountered by a molecular system in thermal equilibrium at several hundred degrees centigrade.

The electric-beam resonance method as originally applied by Hughes did not measure rotational transitions, and hence did not give moments of inertia but rather the product of the dipole moment and the moment of inertia. Although the product μI could be obtained very precisely, the separate values of μ and I could be learned only approximately. Later, however, Lee, Fabricand, Carlson, and Rabi^{3,6} were able to extend the method to the centimeter wave region where the lowest J rotational transitions of a few of the alkali halides could be reached and measured very precisely.

EXPERIMENTAL ASPECTS

Millimeter-Wave and Electronic Components. With the exception of the absorption cell, the spectrometer is very similar to the millimeter and submillimeter wave gaseous spectrometer which has been used for a number of years in this laboratory.⁷ The frequency measurements were made with a secondary standard monitored by the 5 Mc/sec standard frequency broadcast by station WWV, in a manner described by Unterberger and Smith.⁸ The millimeter-wave harmonic generator and detector are those developed and described by King and Gordy.⁹ The fundamental source

* This research was supported by the U. S. Air Force Office of Scientific Research of the Air Research and Development Command.

¹ A. K. Garrison and W. Gordy, *Phys. Rev.* **108**, 899 (1957).

² H. K. Hughes, *Phys. Rev.* **72**, 614 (1947).

³ C. A. Lee, B. P. Fabricand, R. O. Carlson, and I. I. Rabi, *Phys. Rev.* **91**, 1395 (1953).

⁴ M. L. Stitch, A. Honig, and C. H. Townes, *Rev. Sci. Instr.* **25**, 759 (1954).

⁵ A. Honig, M. Mandel, M. L. Stitch, and C. H. Townes, *Phys. Rev.* **96**, 629 (1954).

⁶ B. P. Fabricand, R. O. Carlson, C. A. Lee, and I. I. Rabi, *Phys. Rev.* **91**, 1403 (1953).

⁷ W. C. King and W. Gordy, *Phys. Rev.* **90**, 319 (1953).

⁸ R. R. Unterberger and W. V. Smith, *Rev. Sci. Instr.* **19**, 580 (1948).

⁹ W. C. King and W. Gordy, *Phys. Rev.* **93**, 407 (1954).

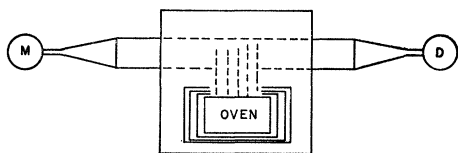


FIG. 1. Sketch showing waveguide cell and molecular-beam source. M and D represent the microwave source and detector, respectively.

was an 8-mm EMI reflex klystron. As a multiplier crystal we employed one of the special silicon crystals developed by Ohl, of the Bell Telephone Laboratories. These crystals and the special treatment to enhance their multiplying characteristics are described by Ohl, Budenstein, and Burrus.¹⁰ We are grateful to C. A. Burrus, now at the Bell Telephone Laboratories, for kindly supplying us with the particular crystals employed in this work.

Absorption Cell. Figure 1 shows the arrangement of the absorption cell. It consists of a section of *S*-band waveguide (dimensions: $2\frac{2}{3}\frac{1}{2} \times 1\frac{1}{2}$ in.) with a slot in the narrow sides to allow the molecules from the oven and the collimator to pass across the cell perpendicularly to the path of radiation. As arranged in the diagram, the molecular path is perpendicular to the *E* vector of the radiation, but this is not essential. Actually, in most experiments a cell was employed which had a slot cut only in the side where the molecules entered the waveguide. They were trapped on the opposite wall of the waveguide cell which was maintained at room temperature. In runs of normal length, the dielectric loss caused by salt collected on the waveguide wall did not become excessive before the end of the run. Thin mica windows used to seal the cell were placed across the small millimeter waveguide at the points of input and output of the cell. These were arranged at a distance of about one foot from the molecular path to prevent scattered molecules from collecting on the windows. Because the large *S*-band guide has little attenuation for millimeter waves, the extra lengths required to achieve clean windows was not costly. To connect the small *G*-band waveguide (0.075×0.034 in.), the output of the harmonic generator, to the large *S*-band waveguide, tapered horns 12 in. in length were employed. These were electroformed in our laboratory.

The chief innovation in the present experiments over the initial one of Garrison and Gordy¹ is the use of the slotted *S*-band guide rather than matched horns with an open space between them, through which the molecules were sprayed. The present cell proved to be more broad banded and easier to use in the search for lines. Also, it seemed to be less lossy for the shorter millimeter waves.

Oven. The oven, enclosed by the radiation shields, was constructed in two parts, each of stainless steel.

The bottom section was prepared from a solid block of steel by hollowing it into a shell with an open top, leaving enough room on the other three sides for drilling several holes the length of the oven. These hold the loosely wound coils of molybdenum wire (0.030 in. in diam) which were insulated from the steel by tubes of high-temperature Vicor glass, or of quartz or thoria ceramic. The latter were needed only for the highest temperatures. These heater coils, connected in series, are joined to Kovar seal terminal posts by means of another pair of posts and strips of stainless steel. The thermocouple lead is mounted loosely next to the oven, and it is insulated and sealed in the bottom plate with an epoxy resin. The Chromel-Alumel thermocouple leads are connected to a Leeds and Northrup potentiometer, where the temperature is read in millivolts. The top section of the oven contains two more heating coils and the collimating apertures, which will be discussed later. The oven is relatively efficient up to temperatures of 700° to 800°C according to the exact condition of the radiation shields and the absence or presence of resistance leaks to ground.

Collimator. For best collimation with maximum cross-sectional beam area, long parallel tubes were stacked in groups. The theory of long parallel tubes for collimating purposes has been fully discussed by Giordmaine and Wang.¹¹ The $\frac{3}{8}$ -in. holes were drilled in the top section as shown in Fig. 2, and each of these was packed with about fifty stainless-steel tubes, $\frac{1}{4}$ in. long, with an inner diameter of 0.015 in. and an outer diameter of 0.020 in. Basically, this type of aperture can be treated just like a channel slit (a slit with a finite depth).¹² The slit or diameter of the tubing should be of the order of the mean free path inside the source. A typical mean free path of an alkali halide at 1 mm pressure of mercury at 1000°C is about 0.010 to 0.020 in. The linewidths which we observed indicate that adequate collimation was present, and the necessary large number of molecules was present in the microwave field.

Precision. In our experiments we chose to compromise the degree of molecular beam collimation to gain in number of molecules passing through the cell. This compromise was justified because our electronic system was not designed to take advantage of excessively sharp lines. Even so, we were able to achieve with ease a factor of precision, $\Delta f/f$, of 10^{-6} as contrasted with the 10^{-4} to 10^{-5} achieved in the earlier hot-cell measurements by the Columbia University group.^{4,5} With a frequency-stabilized klystron and a high-fidelity receiving system, a more highly collimated beam would be justified. With such a system one could achieve a precision factor of 10^{-7} or better, but the measurements would be slower and more tedious. At this stage we

¹¹ J. A. Giordmaine and T. C. Wang, *J. Appl. Phys.* **31**, 463 (1960).

¹² N. F. Ramsey, *Molecular Beams* (Oxford University Press, New York, 1956), pp. 11–25.

¹⁰ R. S. Ohl, P. P. Budenstein, and C. A. Burrus, *Rev. Sci. Instr.* **30**, 765 (1959).

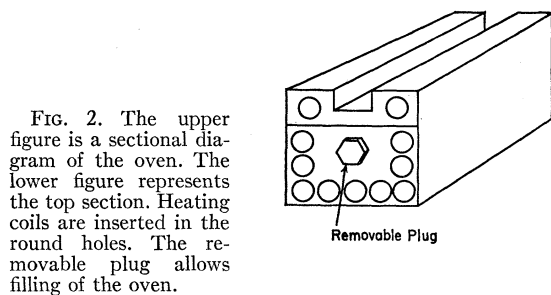
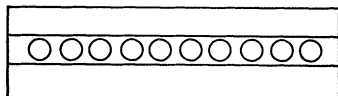


FIG. 2. The upper figure is a sectional diagram of the oven. The lower figure represents the top section. Heating coils are inserted in the round holes. The removable plug allows filling of the oven.



chose to employ the more versatile video-sweep spectrometer with an incompletely collimated molecular beam. In this way we could obtain much new information in a reasonable time. Later, more precise measurements can be made on selected molecules for which the information gained would seem to merit the extra effort.

THEORY

Rotational and Vibrational Constants. Like Honig *et al.*,⁵ we have applied the theory of Dunham¹³ to obtain various molecular constants from the measured rotational frequencies. For clarity, it is necessary to reproduce here certain expressions from this theory. Dunham assumed a potential function represented by the power series,

$$u(r) = a_0\xi^2(1 + a_1\xi + a_2\xi^2 + \dots) + B_v J(J+1)(1 - 2\xi + 3\xi^2 - 4\xi^3 + \dots), \quad (1)$$

where $\xi = (r - r_e)/r_e$, J is the rotational quantum number, and the a 's and B_e are constants. He employed the Wentzel-Kramers-Brillouin method to obtain a solution of the wave equation for the vibrating rotor. The energy eigenvalues which he found are expressed by

$$T_{v,J} = \sum_{i,j} Y_{i,j} (v + \frac{1}{2})^i J^j (J+1)^j, \quad (2)$$

where v is the vibrational quantum number, and where $Y_{i,j}$ are coefficients which depend on the molecular properties. The first few of these coefficients can be directly related to the spectral constants in the more familiar expression for the eigenvalues¹⁴:

$$W_{J,v}/h = \omega_e(v + \frac{1}{2}) - \omega_e x_e(v + \frac{1}{2})^2 + \dots + B_v J(J+1) - D_v J^2(J+1)^2 + \dots + H_v J^3(J+1)^3 + \dots, \quad (3)$$

¹³ J. L. Dunham, Phys. Rev. **41**, 721 (1932).

¹⁴ G. Herzberg, *Molecular Structure and Molecular Spectra* (D. Van Nostrand Company, Inc., Princeton, New Jersey, 1950), Vol. 1, p. 109.

where

$$B_v = B_e - \alpha_e(v + \frac{1}{2}) + \gamma_e(v + \frac{1}{2})^2 + \dots, \quad (4)$$

$$D_v = D_e + \beta_e(v + \frac{1}{2}) + \dots, \quad (5)$$

$$H_v \cong H_e,$$

v =vibrational quantum number, and J =rotational quantum number. These constants are further defined or interrelated by the following equations¹⁴:

$$B_e = h/(8\pi^2 I_e), \quad (6a)$$

$$I_e = \mu r_e^2, \quad (6b)$$

$$D_e = (4B_e^3)/\omega_e^2, \quad (6c)$$

$$\beta_e = D_e \frac{8\omega_e x_e}{\omega_e} - \frac{5\alpha_e}{B_e} - \frac{\alpha_e^2 \omega_e}{24B_e^3}, \quad (6d)$$

$$\alpha_e = 6 \left(\frac{\omega_e x_e B_e^3}{\omega_e^2} \right)^{\frac{1}{2}} - \frac{6B_e^2}{\omega_e}. \quad (6e)$$

Equation (6e) is valid only if the Morse potential¹⁵ is assumed, and is useful for comparison with Dunham's potential. Here, μ is the reduced mass, r_e is the internuclear distance, and I_e is the moment of inertia.

The Y 's in the Dunham potential function are related approximately to these spectral constants by

$$\begin{aligned} Y_{10} &\cong \omega_e, & Y_{01} &\cong B_e, & Y_{11} &\cong -\alpha_e, \\ Y_{20} &\cong -\omega_e x_e, & Y_{02} &\cong -D_e, & Y_{21} &\cong \gamma_e, \\ Y_{03} &\cong H_e, & Y_{12} &\cong -\beta_e. \end{aligned} \quad (7)$$

Usually these approximations are adequate, but in some instances we shall require the more accurate expression for Y_{01} given by Dunham,

$$Y_{01} = B_e(1 + B_e^2 \beta_{01}/\omega_e^2), \quad (8)$$

where

$$\beta_{01} = (Y_{10}^2 Y_{21}/4Y_{01}) + (16a_1 Y_{20}/3Y_{01}) - 8a_1 - 6a_1^2 + 4a_1^3, \quad (9)$$

in which

$$a_1 = (Y_{11} Y_{10}/6Y_{01}^2) - 1. \quad (10)$$

For most of the alkali halides B_e^2/ω_e^2 is usually less than 10^{-6} and β_{01} is small; therefore the above approximation with $Y_{01} = B_e$ is adequate.

Only six of the Dunham coefficients, Y_{01} , Y_{02} , Y_{03} , Y_{11} , Y_{21} , Y_{12} , are necessary for expressing the observed millimeter wave spectra of the alkali halides to the accuracy of our measurements. If the selection rules $\Delta v = 0$ and $\Delta J = +1$ are applied, the frequency equation is

$$\begin{aligned} \nu = 2Y_{01}(J+1) + 2Y_{11}(v + \frac{1}{2})(J+1) + 2Y_{21}(v + \frac{1}{2})^2(J+1) \\ + 4Y_{02}(J+1)^3 + 4Y_{12}(v + \frac{1}{2})(J+1)^3 \\ + Y_{03}(J+1)^3[(J+2)^3 - J^3]. \end{aligned} \quad (11)$$

¹⁵ P. M. Morse, Phys. Rev. **34**, 57 (1929).

Actually, the term in V_{03} is too small to have a measurable effect on most of the transitions which we measured. In no case were we able to measure H_e reliably.

Nuclear Hyperfine Structure. In the above theory nuclear interactions are neglected which must now be considered. Because the electronic ground states of all the alkali halides are nonmagnetic, $^1\Sigma$ states, there is no resolvable nuclear magnetic interactions. However, all the common isotopes of the alkali metals and all the halogens except fluorine have nuclear spins of $\frac{3}{2}$, or greater, and hence have nonvanishing electric quadrupole moments which can give rise to observable splitting of the rotational levels. The stable isotopes of bromine and iodine have relatively large nuclear quadrupole moments. Nevertheless, the nuclear quadrupole couplings in the alkali halides are not large, because the high degree of ionic character in these molecules tends to give the halogen a negatively charged, closed-shell structure which has a too nearly spherically symmetric electronic cloud to give much coupling. The alkali atom has only an s electron in its valence shell and thus tends to have a spherically symmetric cloud about the nuclei whether the bonding is ionic or covalent. In this study we did not observe any nuclear quadrupole effects of the alkali atom, and only in a few instances did we observe the hyperfine structure for the halogen. In these instances, where there was a single nucleus with relatively small coupling in a diatomic molecule, the splitting of the rotational lines could be calculated with first-order perturbation theory. For this simple case the splitting of the rotational levels is given by¹⁶

$$E_Q = -eQq \left[\frac{\frac{3}{4}C(C+1) - I(I+1)J(J+1)}{2I(2I-1)(2J-1)(2J+3)} \right], \quad (12)$$

where

$$\begin{aligned} C &= F(F+1) - I(I+1) - J(J+1), \\ F &= J, J+1, \dots, 1-J, -J, \end{aligned} \quad (13)$$

and where I is the nuclear spin and eQq is the nuclear quadrupole coupling constant, in which Q is the nuclear quadrupole moment and q is the averaged value of $(\partial^2 V)/(\partial z^2)$ for the electrons at the nucleus where z is along the bond axis. The nuclear splitting of the levels decreases rapidly with increasing J . At the high J values observed in the shorter millimeter wave region, the quadrupole splitting is not resolvable for the heavier alkali halides such as CsI, which we studied, even with the high resolution made possible by the molecular beam method. This quadrupole splitting was resolvable for the lighter molecules such as LiI, and broadening of the lines by the unresolved quadrupole interaction was noticeable in some of the heavier molecules for which only high- J transitions were observed. Because we observed only high- J millimeter wave transitions,

we could in no instance obtain an improvement on the quadrupole coupling constants eQq already obtained by Honig *et al.*⁵ with low- J transitions in the centimeter wave region. We have therefore used their values for eQq with the above theory to calculate the expected splitting or broadening of the millimeter wave lines so that corrections for these effects could be made in the evaluation of other molecular constants.

Linewidths. In spectra observed at high temperatures the chief contributions to linewidth are pressure or collision broadening, collision-with-the-wall broadening, and broadening caused by the Doppler effect. Other factors which might be significant are quadrupole broadening and the natural linewidth arising from the uncertainty principle.

Pressure broadening results from collisions between molecules. In a well collimated beam of molecules the number of collisions should be negligible, but when a buffer gas is intentionally introduced there is some of this broadening, which is proportional to the pressure. Collision-with-the-wall broadening is also negligible, but not zero, since the molecule may not always lose enough energy upon the first collision with the wall to condense. Also, there are always some collisions in a molecular beam because of the differing velocities of the molecules.

Much of the line broadening which we encounter here can be attributed to the Doppler effect because an exceptionally well collimated beam of molecules would be required to insure that all the molecules move in a direction normal to the radiation path. Any component of molecular velocity parallel to the incident path of propagation of radiation gives the frequency shift

$$\nu = \nu_0(1 + v/c). \quad (14)$$

Because of symmetry in the molecular beam, this shift results in broadening of the line rather than in a frequency displacement. If a Maxwellian distribution of velocities is assumed, the half-width of the line at half-power points caused by Doppler effects can be shown to be¹⁶

$$\Delta\nu = (7.15/2)10^{-7}\nu_0(T/M)^{\frac{1}{2}}. \quad (15)$$

Although at room temperature in ordinary absorption cells this broadening is usually smaller than collision broadening, it is probably the most important broadening observed in these studies, if nuclear quadrupole effects are neglected. In all the molecules studied here, the Doppler half-widths at 100 kMc/sec would range from 70 to 120 kc/sec, if reductions caused by collimation were not made. It is evident that these Doppler widths have been reduced in our experiment to values less than half those expected for molecules in a normal hot cell.

In estimating the amount of Doppler broadening one must first subtract the broadening caused by unresolved quadrupole structure (which is seldom

¹⁶ W. Gordy, W. V. Smith, and R. F. Trambarulo, *Microwave Spectroscopy* (John Wiley & Sons, Inc., 1953).

negligible) and the natural width caused by the finite time of interaction between the molecule and the radiation field. The latter can be estimated with the uncertainty principle as $\Delta\nu\Delta t \cong h$. For a typical molecule in these experiments this type of broadening is of the order of 5 to 10 kc/sec.

Analysis of Data. The data were treated by the following, least-square method. After the line frequencies have been corrected for the Y_{03} term, the remaining set of equations is

$$f_i(Y_{01}, Y_{02}, Y_{11}, Y_{21}, Y_{12}) = 0, \quad (16)$$

where i equals the number of equations or measurements made on a molecule. If $F = \sum_i f_i^2$, the i equations can be reduced to the five normal equations,

$$(\partial F / \partial Y_{j,k}) = 0, \quad (17)$$

which minimizes the sum of the errors squared. When solved, these five equations will give the least-square solutions to the five Y 's. Since, in the process of solving for some of the constants, differences of very large numbers are taken which give very small answers, it is desirable to keep ten significant figures through the calculations. By use of the Crout method,¹⁷ which takes advantage of the characteristics of the typical desk calculator, these calculations can be made quickly.

The accuracy quoted on these mean values is based on a calculation of the "standard error of the mean." With ten to twenty measurements on a molecule, over 90% of the measured frequencies would fall within 2α of the least-square value, where α is the standard error of the line frequency, which is found by use of¹⁸

$$\alpha^2 = [dd]/(i-m), \quad (18)$$

where i is the number of equations, m is the number of unknowns, and $[dd]$ is the sum of the squares of the deviations of the measured line frequencies from the calculated ones. The standard error of a particular Y can be found from¹⁸

$$\alpha_m^2 = [a_{mn}]^2 \alpha^2 / \Delta, \quad (19)$$

where α_m is the standard error of Y_m , $[a_{mn}]$ is the 4×4 determinant obtained when perpendicular lines are drawn through the coefficient a_{mn} corresponding to the Y_{mn} , and where Δ is the 5×5 determinant of all the coefficients.

EXPERIMENTAL RESULTS

Millimeter wave spectra have been obtained for all the common isotopes of ten alkali metal bromides and iodides. The important points about each molecule are summarized in succeeding paragraphs, and tables are given for each molecule showing all measured, derived, and extrapolated constants, as well as com-

parisons with the best previously known data. Also given for each molecule is a listing of all measured line frequencies and all calculated ones. The latter were based on a least-square solution of each set of measurements. Reagent-grade salts were used in every instance.

Lithium Bromide. Lithium bromide is the lightest molecule of the group. Since the frequency range of all observations is set by necessity, the lowest J levels observed are for the lightest molecule. As was noted in the theoretical discussion, low J values show the greatest nuclear quadrupole effects. Bromine 79 of $\text{Li}^7\text{Br}^{79}$ has a quadrupole coupling constant eQq of $+37.20 \pm 0.45$ Mc/sec in the ground vibrational state.⁵ Although the nuclear spin of Li^7 is $\frac{3}{2}$, the coupling with J is so small that it has not been observed. Bromine 81 has a coupling constant of $+30.71 \pm 0.40$ Mc/sec. Since both bromine isotopes have a nuclear spin of $\frac{3}{2}$, the energy-level structures are similar, though they differ somewhat in the magnitude of their splittings. The nuclear quadrupole interaction splits each J level into $(2I+1)$ levels, or four levels for a spin of $\frac{3}{2}$. These levels are designated with the F quantum number which varies in integral steps from $(J+\frac{3}{2})$ to $J-\frac{3}{2}$. If pure rotational transitions are assumed, the selection rules allow for the transitions $\Delta J = +1$ and $\Delta F = 0, \pm 1$. Of the four strong lines corresponding to $\Delta F = +1$, only a doublet was observed, because each of the lines is a degenerate pair.

As shown in Table I, three transitions were studied

TABLE I. Lithium bromide ($\text{Li}^7\text{Br}^{79}$).

Present results		Previous results	
$Y_{01}^a =$	$16\ 650.318 \pm 0.06$	$16\ 650.570 \pm 0.05^b$	Mc/sec
$B_0^a =$	$16\ 650.179 \pm 0.10$	$16\ 651.186 \pm 0.05^b$	Mc/sec
$B_0^b =$	$16\ 565.9369 \pm 0.006$		Mc/sec
$D_0 =$	64.705 ± 0.12		kc/sec
$\alpha_e = -Y_{11} =$		169.09 ± 0.08^b	Mc/sec
$\gamma_e = Y_{21} =$		656 ± 40^b	kc/sec
$D_e^a = -Y_{02} =$	64.71 ± 0.25		kc/sec
$eQq/h =$		$+37.20 \pm 0.45^b$	Mc/sec
Derived constants		Previous constants	
$\omega_e = Y_{10} =$	563.5 ± 2.2	$480^{b,c}$	cm^{-1}
$\omega_e x_e = -Y_{20} =$	3.88 ± 0.02^c	1.7^c	cm^{-1}
$I_e =$	30.3618 ± 0.0011	30.36012^b	$\text{amu } \text{Å}^2$
$r_e =$	2.17042 ± 0.00004	2.1704 ± 0.0001^b	Å
Transitions $v=0$		Measured lines	Calculated lines
$J=2-3$	$\left\{ \begin{array}{l} F=7/2-9/2 \\ F=5/2-7/2 \end{array} \right\}$	$99\ 388.21 \pm 0.10$	$99\ 388.19$ Mc/sec
	$\left\{ \begin{array}{l} F=3/2-5/2 \\ F=1/2-3/2 \end{array} \right\}$	$99\ 390.39 \pm 0.20$	$99\ 390.49$ Mc/sec
$J=3-4$	$\left\{ \begin{array}{l} F=9/2-11/2 \\ F=7/2-9/2 \end{array} \right\}$	$132\ 510.64 \pm 0.10$	$132\ 510.65$ Mc/sec
	$\left\{ \begin{array}{l} F=5/2-7/2 \\ F=3/2-5/2 \end{array} \right\}$	$132\ 511.83 \pm 0.20$	$132\ 511.73$ Mc/sec
$J=5-6$	not resolved	$198\ 735.33 \pm 0.20$	$198\ 735.34$ Mc/sec

^a Extrapolated from other constants.

^b Honig *et al.*, see reference 5.

^c Theoretical values.

¹⁷ K. S. Kunz, *Numerical Analysis* (McGraw-Hill Book Company, Inc., New York, 1957), pp. 226-229.

¹⁸ J. Topping, *Errors of Observation and their Treatment* (Institute of Physics, London, 1955), pp. 99-112.

TABLE II. Lithium bromide ($\text{Li}^7\text{Br}^{81}$).

Present results		Previous results	
$Y_{01}^a = 16\,616.780 \pm 0.07$		$16\,617.002 \pm 0.05^b$	Mc/sec
$B_e^a = 16\,616.622 \pm 0.13$		$16\,617.617 \pm 0.05^b$	Mc/sec
$B_0 = 16\,532.653 \pm 0.02$			Mc/sec
$D_0 = 64.8 \pm 1.7$			kc/sec
$\alpha_e = -Y_{11} =$		168.58 ± 0.08^b	Mc/sec
$\gamma_e = Y_{21} =$		653 ± 40^b	kc/sec
$D_e^a = -Y_{02} = 64.8 \pm 1.7$			kc/sec
$eQq/h =$		30.71 ± 0.40^b	Mc/sec
Derived constants		Previous constants	
$\omega_e = Y_{10} = 561 \pm 15^c$			cm^{-1}
$\omega_e x_e = -Y_{20} = 3.86 \pm 0.1^c$			cm^{-1}
$I_e = 30.4232 \pm 0.0011$			$\text{amu } \text{Å}^2$
$r_e = 2.17042 \pm 0.00004$			Å
Transitions $v=0$		Measured lines	Calculated lines
$J=4-5 \left\{ \begin{array}{l} F=11/2-13/2 \\ F=9/2-11/2 \end{array} \right.$	$165\,294.10 \pm 0.20$	same	Mc/sec
$J=5-6$	$198\,335.75 \pm 0.20$	same	Mc/sec

^a Extrapolated from other constants.

^b Honig *et al.*, see reference 5.

^c Theoretical estimates.

in the 79 isotope; two more were studied in the 81 isotope (see Table II). Contrary to expectation, the quadrupole structure of the $J=5 \rightarrow 6$ transition was not resolved but appeared as a broad line of medium strength. This may be due to the presence of water vapor in the beam which broadened the lines sufficiently to prevent resolution of the structure. The $J=4 \rightarrow 5$ transitions were especially hard to observe because both the resolvable hyperfine splitting and the decrease in intensity with the cube of frequency make the lines weak in comparison with the $J=5 \rightarrow 6$ transition. Both transitions were observed with fifth harmonic power from the harmonic generator.

No excited vibrational states were observed for LiBr although the Boltzmann distribution indicates that the population of $v=1$ states in LiBr should be down only 56% from the ground state at the temperature required for vaporization. Possibly the effective temperature in the observed molecular beam was considerably lower than the source temperature. This effect was noticed mainly in the lithium salts. It may be caused by collisions of the salt molecules with cooler water vapor molecules which evaporated from the salt and formed a cloud in the cell. There was evidence that the sample used contained water of crystallization. Because no excited vibrational states were measured, only B_0 and D_0 could be obtained. The value of B_e was extrapolated from the values of Y_{11} and Y_{21} , as measured by Honig *et al.*,⁵ although there is some doubt about their accuracy. The value of D_0 was assumed to be approximately equal to that of D_e . This assumption is based on the fact that, in all the other molecules studied, the value of β_e was never more than 1/500 as large as that of D_e . This assumption was also used in the derivation of ω_e and $\omega_e x_e$. Our value of B_e deviates

by more than twice the sum of the estimated error from the value obtained by Honig *et al.* The reason for this deviation is not known.

Lithium Iodide. In lithium iodide the I^{127} nucleus gave rise to an observable hyperfine structure of its millimeter wave rotational spectra, but again effects of the lithium nuclear interaction were not detectable. The value of eQq for I^{127} in LiI is -198.15 Mc/sec.⁵ Because the nuclear spin of iodine is $\frac{5}{2}$, each J level is split into six components. With the selection rules for F , this gives a possibility for 15 lines, although at the J levels studied only the $\Delta F = +1$ lines are of significant strength.

Table III^{5,19} gives the observed and theoretical spectrum for $J=6 \rightarrow 7$, $\Delta F = +1$. These and the $J=5 \rightarrow 6$ lines were measured. As an example of the weaker transitions not measured, the strongest $\Delta F = 0$ line in the $J=6 \rightarrow 7$ spectrum should be down by a factor of 7 from the weakest $\Delta F = +1$ line, and the strongest $\Delta F = -1$ line down by a factor of 300. The spectrum for $\Delta F = 1$ was completely resolved, except for the narrow separation of 0.25 Mc/sec, which was barely visible.

As for LiBr, only B_0 and D_0 were measured directly. The equilibrium constants B_e and D_e were evaluated from them (see Table III) with the aid of the data by

TABLE III. Lithium iodide ($\text{Li}^7\text{I}^{127}$).

Present results		Previous results	
$Y_{01}^a = 13\,286.262 \pm 0.07$		$13\,286.386 \pm 0.08^b$	Mc/sec
$B_e^a = 13\,286.15 \pm 0.10$		$13\,286.785 \pm 0.08^b$	Mc/sec
$B_0 = 13\,225.066 \pm 0.011$			Mc/sec
$D_0 = 43.41 \pm 0.13$			kc/sec
$\alpha_e = -Y_{11} =$		122.62 ± 0.10^b	Mc/sec
$\gamma_e = Y_{21} =$		455 ± 50^b	kc/sec
$D_e^a = -Y_{02} = 43.41 \pm 0.25$			kc/sec
$eQq/h =$		-198.15 ± 0.30^b	Mc/sec
Derived constants		Previous constants	
$\omega_e = Y_{10} = 490 \pm 14^c$		450^d	cm^{-1}
$\omega_e x_e = -Y_{20} = 3.1 \pm 0.1^c$		1.5^d	cm^{-1}
$I_e = 38.0494 \pm 0.0013$		38.04799^b	$\text{amu } \text{Å}^2$
$r_e = 2.39191 \pm 0.00004$		2.3919 ± 0.0001^b	Å
Transitions $v=0$		Measured lines (Mc/sec)	Calculated lines (Mc/sec)
$J=5-6$	$F=13/2-15/2$	$158\,664.68 \pm 0.20$	158 664.66
	$F=15/2-17/2$	158 664.12	158 664.06
	$F=11/2-13/2$	158 663.12	158 663.15
	$F=5/2-7/2$	158 662.00	158 661.91
	$F=9/2-11/2$	158 661.28	158 661.31
	$F=7/2-9/2$	158 660.44	158 660.57
$J=6-7$	$F=15/2-17/2$	$185\,092.51 \pm 0.20$	185 092.42
	$F=17/2-19/2$	185 091.98	185 091.95
	$F=13/2-15/2$	185 091.31	185 091.38
$F=11/2-13/2, 7/2-9/2$		185 090.17	185 090.21
	$F=9/2-11/2$	185 089.47	185 089.50

^a Extrapolated from other constants.

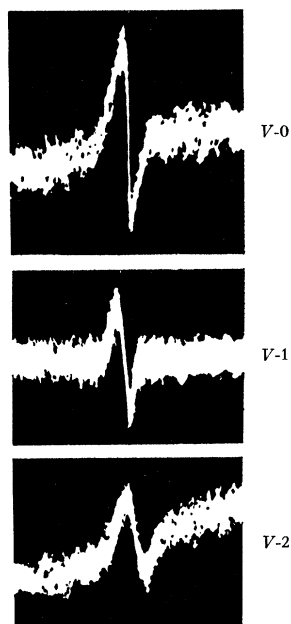
^b Honig *et al.*, see reference 5.

^c Theoretical estimates.

^d Levi, see reference 19.

¹⁹ H. Levi, dissertation, Berlin, 1934 (unpublished, quoted in reference 5, p. 634).

FIG. 3. The $J=20 \rightarrow 21$ transition of NaBr^{79} at 187 kMc/sec (1.6-mm wavelength) in the ground vibrational state and in the first and second excited vibrational states. The lines are about 100 kc/sec in width and are distorted by the amplifier because of the rapid sweep used.



Honig *et al.*⁵ For LiI and in fact for all the molecules in this study except RbBr, the Y_{01} value is lower than that obtained by Honig *et al.*, but is within the limits of their standard errors.

From the line intensities it seems that LiBr, and to a lesser extent LiI, contain a moderate percentage of dimers in the beam. From work done here and other laboratories,²⁰ it appears that all the alkali halides which are as light as, or lighter than, NaCl may contain at least 50% dimers.

The lithium halides were the most difficult of the present group for experimental handling. Both of them are very deliquescent and release their water molecules at a temperature of about 50°C.²¹ Thus, these salts, which cannot be obtained in a purely anhydrous form, must be warmed very slowly so that all the water will be pumped away. When the temperature suitable for the beam has been reached, water may be released so rapidly from some of the Lavite spacers and insulators that the vacuum deteriorates too quickly for observation of transitions to be attempted. This condition can be avoided with these two salts only if the Lavite is washed free of all traces of salt after each run and is baked in a very hot furnace for several hours so that no water attracted by the salt and reabsorbed by the Lavite will remain.

These two salts, again, partly because of their deliquescence, are the most difficult to remove from the interior walls of the S-band wave guide. The drier salts tend to flake off when scraped, and the remaining

powder is very soluble in water. The spectra of LiI were first observed at a temperature of 600°C.

Sodium Bromide. Sodium bromide is a good illustration of a molecule that is best studied at either rather high, or at very low, microwave frequencies. The coupling of the nucleus of bromine with J , eQq of +58 Mc/sec, produces just enough splitting at 24 kMc/sec frequency for the lines with the hot cell to be very broad but not resolvable.⁵ At 100 kMc/sec the quadrupole broadening is 180 kc/sec, enough to limit only slightly the accuracy of the measurements. At higher frequencies this broadening becomes negligible. Examples of some lines measured are given in Fig. 3. There one sees a relative comparison of three vibrational transitions at approximately 1.6-mm wavelength (187 kMc/sec). The lines are sharp, with no evidence of the unresolved hyperfine structure.

An evaluation of five Y 's was made (see Tables IV and V). All of them, even the vibration-rotation interaction constants, were obtained much more accurately than in the earlier work of Honig *et al.* The H_e term was found to be negligible in all of the measurements. The stretching constant D_e , which had been assumed to be about 7 kc/sec,⁵ was found to be 50% too high; this accounts for the value of Y_{01} , which is larger than expected. The ratio of the mass isotopes of bromine is larger than expected in comparison with the other determinations of that quantity, although within the error limits. The spectra were first observed at a temperature of 740°C.

Sodium Iodide. Sodium iodide is the only other

TABLE IV. Sodium bromide ($\text{Na}^{23}\text{Br}^{79}$).

Present results		Previous results	
$Y_{01} =$	4534.4603 ± 0.0032	4534.51 ± 0.10^a	Mc/sec
$B_e =$	4534.4658 ± 0.0072	4534.52 ± 0.10^a	Mc/sec
$\alpha_e = -Y_{11} =$	28.2091 ± 0.0038	28.25 ± 0.10^a	Mc/sec
$\gamma_e = Y_{21} =$	72.92 ± 1.2	85 ± 30^a	kc/sec
$D_e = -Y_{02} =$	4.6574 ± 0.0054	7 ± 3^a	kc/sec
$\beta_e = -Y_{12} =$	-0.0149 ± 0.0028		kc/sec
Derived constants		Previous constants	
$\omega_e = Y_{10} =$	298.49 ± 0.17	315^b	cm^{-1}
$\omega_e x_e = -Y_{20} =$	1.16 ± 0.03	1.15^b	cm^{-1}
$I_e =$	111.486 ± 0.004	111.486^a	$\text{amu } \text{Å}^2$
$r_e =$	2.50201 ± 0.00004	2.5020 ± 0.0001^a	Å
Transitions		Measured lines (Mc/sec)	Calculated lines (Mc/sec)
$v=0$	$J=11-12$	$108\ 456.85 \pm 0.10$	108 456.84
	$J=12-13$	117 488.93	117 488.86
	$J=15-16$	144 575.72	144 575.78
	$J=16-17$	153 601.28	153 601.34
	$J=20-21$	189 683.49	189 683.46
$v=1$	$J=11-12$	$107\ 783.39 \pm 0.10$	107 783.42
	$J=12-13$	116 759.38	116 759.35
	$J=20-21$	188 505.34	188 505.35
$v=2$	$J=12-13$	$116\ 033.62 \pm 0.10$	116 033.62
	$J=20-21$	187 333.37	187 333.37

^a Honig *et al.*, see reference 5.

^b Levi, see reference 19.

²⁰ S. A. Ochs, R. E. Cote, and P. Kusch, *J. Chem. Phys.* **21**, 459, (1953).

²¹ S. D. Hodgman, R. C. West, and S. M. Selby, *Handbook of Chemistry and Physics* (Chemical Rubber Publishing Company, Cleveland, Ohio, 1958), 39th ed., p. 548.

TABLE V. Sodium bromide ($\text{Na}^{23}\text{Br}^{81}$).

Present results		Previous results	
$B_e =$	$Y_{01} = 4509.1958 \pm 0.0055$	4509.34 ± 0.10^a	Mc/sec
$\alpha_e = -Y_{11} =$	27.9688 ± 0.0066	28.06 ± 0.10^a	Mc/sec
$\gamma_e = Y_{21} =$	71.37 ± 1.6		kc/sec
$D_e = -Y_{02} =$	4.5950 ± 0.0070		kc/sec
$\beta_e = -Y_{12} =$	-0.0087 ± 0.0062		kc/sec
Derived constants		Previous constants	
$\omega_e = Y_{10} =$	298.00 ± 0.22		cm^{-1}
$\omega_e x_e = -Y_{20} =$	1.20 ± 0.05		cm^{-1}
$I_e =$	112.111 ± 0.004		$\text{amu } \text{Å}^2$
$r_e =$	2.50201 ± 0.00004		Å
Transitions		Measured lines (Mc/sec)	Calculated lines (Mc/sec)
$v=0$	$J=11-12$	$107\ 853.84 \pm 0.10$	107 853.77
	$J=12-13$	116 835.58	116 835.62
	$J=16-17$	152 747.53	152 747.58
	$J=19-20$	179 662.30	179 662.27
	$J=20-21$	188 629.57	188 629.58
$v=1$	$J=11-12$	107 186.03	107 186.01
	$J=12-13$	116 112.12	116 112.22
	$J=16-17$	151 801.77	151 801.67
	$J=19-20$	178 549.47	178 549.51
	$J=20-21$	187 461.19	187 461.20
$v=2$	$J=16-17$	150 860.60	150 860.60

^a Honig *et al.*, see reference 5.TABLE VI. Sodium iodide ($\text{Na}^{23}\text{I}^{127}$).

Present results		Previous results	
$B_e =$	$Y_{01} = 3531.7232 \pm 0.0043$	3531.759 ± 0.035^a	Mc/sec
$\alpha_e =$	19.4198 ± 0.0052	19.439 ± 0.030^a	Mc/sec
$\gamma_e = Y_{21} =$	42.9 ± 1.6	46.9 ± 6.0^a	kc/sec
$D_e = -Y_{02} =$	2.9183 ± 0.0036		kc/sec
$\beta_e = -Y_{12} =$	-0.0014 ± 0.0022		kc/sec
Derived constants		Previous constants	
$\omega_e = Y_{10} =$	259.20 ± 0.16	286 ^b	cm^{-1}
$\omega_e x_e = -Y_{20} =$	0.964 ± 0.024	0.75 ^b	cm^{-1}
$I_e =$	143.140 ± 0.005	143.138 ^a	$\text{amu } \text{Å}^2$
$r_e =$	2.71143 ± 0.00004	2.7115 ± 0.0001^a	Å
Transitions		Measured lines (Mc/sec)	Calculated lines (Mc/sec)
$v=0$	$J=13-14$	$98\ 584.60 \pm 0.20$	98 584.65
	$J=14-15$	105 621.23	105 621.33
	$J=15-16$	112 656.83	112 656.97
	$J=19-20$	$140\ 787.59 \pm 0.10$	140 787.60
	$J=24-25$	175 918.87	175 918.87
	$J=26-27$	189 959.62	189 959.59
$v=1$	$J=13-14$	$98\ 043.38 \pm 0.20$	98 043.31
	$J=14-15$	105 041.57	105 041.33
	$J=15-16$	112 038.42	112 038.30
	$J=24-25$	$174\ 952.22 \pm 0.10$	174 952.23
	$J=26-27$	188 915.62	188 915.66
	$v=2$	$J=13-14$	$97\ 504.24 \pm 0.20$
$J=14-15$		104 463.92	104 463.90
$J=24-25$		$173\ 989.84 \pm 0.10$	173 989.91
$J=26-27$		187 876.42	187 876.36

^a Honig *et al.*, see reference 5.^b Levi, see reference 19.

molecule studied which has a significant amount of quadrupole coupling at the J values observed. It has the largest quadrupole coupling of any of the alkali halides, with an $I^{127} eQq$ of -259.87 Mc/sec.⁵ The $J=13 \rightarrow 14$ transition, which is the lowest frequency observed, has a quadrupole broadening of 900 kc/sec while at the $J=19 \rightarrow 20$ transition this broadening is only 400 kc/sec.

Evaluation of five Y 's was made. The H_e correction was unnecessary. Results are more accurate than previously available ones; D_e and β_e were measured for the first time. A summary of the results is given in Table VI. Lines were first observed at a source temperature of about 660°C. This salt was deliquescent, and some of the precautions mentioned earlier had to be taken.

Potassium Bromide. Fabricand *et al.*,⁶ using molecular beam electric resonance (MBER), have already made very accurate evaluations of Y_{01} , Y_{11} , and Y_{21} for KBr. Several millimeter wave transitions were nevertheless observed in both isotopic species so that Y_{02} and Y_{12} might be measured very carefully. The centrifugal stretching constant D_e was evaluated separately for each isotopic species, but an average solution for β_e was made for both isotopic species, with the isotopic correction taken into account. For this molecule and for CsI, evaluation of β_e is more accurate than it is for the other molecules. Tables VII and VIII give a summary of the results obtained. The derivation of $\omega_e x_e$ from β_e shows that a more accurate value of β_{01} is possible now than before. Previously, the error of

TABLE VII. Potassium bromide ($\text{K}^{39}\text{Br}^{79}$).

Present results		Previous results	
$B_e =$	$Y_{01} = 2434.945 \pm 0.002$	2434.947 ± 0.001^a	Mc/sec
$\alpha_e = -Y_{11} =$		2434.953 ± 0.001^a	Mc/sec
$\gamma_e = Y_{21} =$		12.136 ± 0.001^a	Mc/sec
$D_e = -Y_{02} =$	1.33763 ± 0.00034	23 ± 1^a	kc/sec
$\beta_e = -Y_{12} =$	-0.00006 ± 0.00021		kc/sec
$H_e = Y_{03} =$	-170^b		10^{-6} cps
Derived constants		Previous constants	
$\omega_e = Y_{10} =$	219.170 ± 0.029	230 ^{c,d}	cm^{-1}
$\omega_e x_e = -Y_{20} =$	0.758 ± 0.005	0.7 ^{c,d}	cm^{-1}
$I_e =$		203.4372 ^a	$\text{amu } \text{Å}^2$
$r_e =$	2.82075 ± 0.00005	2.8207 ± 0.0001^a	Å
Transitions		Measured lines (Mc/sec)	Calculated lines (Mc/sec)
$v=0$	$J=20-21$	$101\ 963.70 \pm 0.10$	101 963.79
	$J=21-22$	106 813.95	106 813.94
	$J=31-32$	155 273.22	155 273.18
	$J=39-40$	193 968.20	193 968.16
$v=1$	$J=20-21$	$101\ 455.71 \pm 0.10$	101 455.60
	$J=31-32$	154 499.55	154 499.59
	$J=39-40$	193 001.15	193 001.25
$v=2$	$J=39-40$	$192\ 037.50 \pm 0.10$	192 037.45

^a Fabricand *et al.*, see reference 6.^c Levi, see reference 19.^b Theoretical estimate.^d Barrow and Caunt, see reference 25.

the B_e term was seven times the error of Y_{01} , mainly because of the uncertainty in $\omega_e x_e$. Potassium bromide is the lightest molecule for which we detected effects of the H_e term. At 1.5 mm, effects of this term were of the order of the estimated error of the line frequency measurement.

Potassium Iodide. Potassium iodide has been studied in the first three vibrational states. Again five Y 's have been found. The values for Y_{01} and B_e were learned with 30 times the accuracy of the previous values. Our values for the vibrational constants α_e and γ_e are less accurate than the previous ones by Honig *et al.*⁵ but fall within the sum of the two estimated errors. Our more accurate evaluation of D_e shows that the value given by Honig *et al.* is 30% too large, but the correct value falls within their estimated error limits. They were able to measure α_e and γ_e better than we because they observed rotational transitions in vibrational levels up to $v=7$. Line broadening by nuclear quadrupole interaction in KBr is only 56 kc/sec at 3 mm wavelength. The spectra of this molecule were first observed at a temperature of about 740°C. Table IX gives a summary of the results we obtained.

Rubidium Bromide. Rubidium bromide with its combination of four common isotopic species has the most complicated spectra of all the molecules studied. By chance, the stretching constant obtained by Honig *et al.*⁵ and estimated to only 50% accuracy is within 1% of the correct value. Again, the five Y 's were found after the H_e correction was made. All the Y 's were obtained more accurately for Rb⁸⁵Br⁷⁹ than were previously known. The isotopic species Rb⁸⁵Br⁸¹ was solved for the first time. Since only the ground vibrational state was examined for Rb⁸⁷Br⁷⁹, only a B_0 and a D_0 were measured directly. By extrapolation, with α_e obtained from Honig

et al. and with γ_e and β_e obtained from mass ratios, B_e and D_e were found. An accurate evaluation of the Br⁷⁹/Br⁸¹ mass ratio was obtained with this molecule. The spectra were first detected at the temperature of 690°C. Tables X, XI, and XII give a summary of the results.

Rubidium Iodide. The spectra of both Rb⁸⁵I and Rb⁸⁷I were examined. Although B_e and D_e were found much more accurately than previously known, the α_e and γ_e values of Honig *et al.*⁵ could not be improved. This molecule would be a good one to use for a very accurate determination of the mass ratio of the rubidium isotopes if many more transitions were observed with great care. The spectra were first observed at a temperature of 690°C. Results are summarized in Tables XIII and XIV.

Cesium Bromide. The spectra of cesium bromide were fully investigated. It was the only molecule for which five vibrational states were observed. As a result, the CsBr⁷⁹ analysis gives the most accurate results of the set of vibration-rotation interaction constants, α_e , γ_e , and β_e . Hence, more information is obtained about the potential function. The mass ratio of the bromine isotopes, comparable in accuracy to that obtained from RbBr, is in very close agreement with the RbBr value. All five Y 's were obtained accurately for both isotopes.

TABLE VIII. Potassium bromide (K³⁹Br⁸¹).

Present results		Previous results	
$Y_{01} =$	2415.075 ± 0.001^a Mc/sec	2415.075 ± 0.001^a Mc/sec	
$B_e =$	2415.073 ± 0.002	2415.089 ± 0.007^a Mc/sec	
$\alpha_e = -Y_{11} =$	11.987 ± 0.001^a Mc/sec	11.987 ± 0.001^a Mc/sec	
$\gamma_e = Y_{21} =$	22 ± 1^a kc/sec	22 ± 1^a kc/sec	
$D_e = -Y_{02} =$	1.31593 ± 0.00012		kc/sec
$\beta_e = -Y_{12} =$	-0.00006 ± 0.00021		kc/sec
$H_e = Y_{03} =$	-170^b		10^{-6} cps
Derived constants		Previous constants	
$\omega_e = Y_{10} =$	218.271 ± 0.010 cm ⁻¹		cm ⁻¹
$\omega_e x_e = -Y_{20} =$	0.752 ± 0.005^b cm ⁻¹		cm ⁻¹
$I_e =$	209.323 ± 0.007 amu Å ²		amu Å ²
$r_e =$	2.82075 ± 0.00005 Å		Å
Transitions		Measured lines (Mc/sec)	Calculated lines (Mc/sec)
$v=0$	$J=20-21$	$101\ 132.87 \pm 0.10$	101 132.84
	$J=21-22$	105 943.73	105 943.68
	$J=31-32$	154 009.07	154 009.08
	$J=39-40$	192 389.96	192 389.97

^a Fabricand *et al.*, see reference 6.^b Theoretical estimates.TABLE IX. Potassium iodide (K³⁹I¹²⁷).

Present results		Previous results	
$Y_{01} =$	1824.9786 ± 0.0013	1825.006 ± 0.030^a Mc/sec	Mc/sec
$B_e =$	1824.9778 ± 0.0014	1825.012 ± 0.030^a Mc/sec	Mc/sec
$\alpha_e = -Y_{11} =$	8.0272 ± 0.0015	8.0337 ± 0.0018^a Mc/sec	Mc/sec
$\gamma_e = Y_{21} =$	11.62 ± 0.39	12.21 ± 0.25^a kc/sec	kc/sec
$D_e = -Y_{02} =$	0.77749 ± 0.00031	1.03 ± 0.3^a kc/sec	kc/sec
$\beta_e = -Y_{12} =$	0.00013 ± 0.00018		kc/sec
$H_e = Y_{03} =$	-80^b		10^{-6} cps
Derived constants		Previous constants	
$\omega_e = Y_{10} =$	186.53 ± 0.04	$200^{a,c,d}$	cm ⁻¹
$\omega_e x_e = -Y_{20} =$	0.574 ± 0.006	0.5	cm ⁻¹
$I_e =$	277.006 ± 0.010	277.00945^a	amu Å ²
$r_e =$	3.04781 ± 0.00005	3.0478 ± 0.0001^a Å	Å
Transitions		Measured lines (Mc/sec)	Calculated lines (Mc/sec)
$v=0$	$J=26-27$	$98\ 271.00 \pm 0.10$	98 271.06
	$J=28-29$	105 540.31	105 540.30
	$J=29-30$	109 174.23	109 174.12
	$J=39-40$	145 478.34	145 478.38
	$J=49-50$	181 707.95	181 707.96
$v=1$	$J=26-27$	$97\ 838.77 \pm 0.10$	97 838.84
	$J=28-29$	105 076.04	105 076.06
	$J=29-30$	108 693.88	108 693.87
	$J=39-40$	144 838.07	144 838.02
	$J=49-50$	180 907.50	180 907.50
$v=2$	$J=26-27$	$97\ 407.94 \pm 0.10$	97 407.87
	$J=28-29$	104 613.14	104 613.16
	$J=29-30$	108 214.97	108 215.01
	$J=39-40$	144 838.07	144 838.02
	$J=49-50$	180 109.35	180 109.63

^a Honig *et al.*, see reference 5.^c Levi, see reference 19.^b Theoretical estimates.^d Barrow and Caunt, see reference 25.

TABLE X. Rubidium bromide (Rb⁸⁵Br⁷⁹).

Present results		Previous results	
$Y_{01} =$	1424.8523 ± 0.0012	1424.8342 ± 0.02^a	Mc/sec
$B_e =$	1424.8522 ± 0.0016	1424.840 ± 0.02^a	Mc/sec
$\alpha_e = -Y_{11} =$	5.5760 ± 0.0012	5.5782 ± 0.0056^a	Mc/sec
$\gamma_e = Y_{21} =$	6.83 ± 0.32	7.9 ± 1.1^a	kc/sec
$D_e = -Y_{02} =$	0.44833 ± 0.00016	0.45 ± 0.20^a	kc/sec
$\beta_e = -Y_{12} =$	0.00000 ± 0.00015		kc/sec
$H_e = Y_{02} =$	-46^b		10^{-6} cps
Derived constants		Previous constants	
$\omega_e = Y_{10} =$	169.46 ± 0.03	$181^{a,c}$	cm^{-1}
$\omega_e x_e = -Y_{20} =$	0.463 ± 0.007	0.35^c	cm^{-1}
$I_e =$	354.795 ± 0.012	354.8006^a	$\text{amu } \text{Å}^2$
$r_e =$	2.94471 ± 0.00005	2.9448 ± 0.0001^a	Å
Transitions		Measured lines (Mc/sec)	Calculated lines (Mc/sec)
$v=0$	$J=49-50$	$141\ 982.40 \pm 0.10$	$141\ 982.35$
	$J=50-51$	$144\ 812.72$	$144\ 812.75$
	$J=54-55$	$156\ 128.74$	$156\ 128.76$
	$J=62-63$	$178\ 731.66$	$178\ 731.63$
	$J=68-69$	$195\ 655.53$	$195\ 655.56$
$v=1$	$J=50-51$	$144\ 245.34 \pm 0.10$	$144\ 245.39$
	$J=63-64$	$180\ 842.11$	$180\ 842.07$
	$J=68-69$	$194\ 887.95$	$194\ 887.96$
$v=2$	$J=63-64$	$180\ 131.87 \pm 0.10$	$180\ 131.83$
	$J=68-69$	$194\ 122.20$	$194\ 122.24$

^a Honig *et al.*, see reference 5. ^c Barrow and Caunt, see reference 25.
^b Theoretical estimate.

The spectra were first observed at a temperature of about 650°C. Tables XV and XVI give the results for cesium bromide.

TABLE XI. Rubidium bromide (Rb⁸⁵Br⁸¹).

Present results		Previous results	
$Y_{01} =$	1406.6192 ± 0.0037	1406.5944 ± 0.02^a	Mc/sec
$B_e =$	1406.6192 ± 0.0043		Mc/sec
$\alpha_e = -Y_{11} =$	5.4667 ± 0.0043	5.461 ± 0.011^a	Mc/sec
$\gamma_e = Y_{12} =$	5.71 ± 1.2		kc/sec
$D_e = -Y_{02} =$	0.43722 ± 0.00044		kc/sec
$\beta_e = -Y_{12} =$	0.00001 ± 0.00012		kc/sec
$H_e = Y_{03} =$	-44^b		10^{-6} cps
Derived constants		Previous constants	
$\omega_e = Y_{10} =$	168.32 ± 0.06		cm^{-1}
$\omega_e x_e = -Y_{20} =$	0.459 ± 0.006		cm^{-1}
$I_e =$	359.394 ± 0.012		$\text{amu } \text{Å}^2$
$r_e =$	2.94471 ± 0.00005		Å
Transitions		Measured lines (Mc/sec)	Calculated lines (Mc/sec)
$v=0$	$J=50-51$	$142\ 964.40 \pm 0.10$	$142\ 964.42$
	$J=55-56$	$156\ 928.04$	$156\ 928.10$
	$J=63-64$	$179\ 238.80$	$179\ 238.83$
	$J=69-70$	$195\ 943.97$	$195\ 943.91$
$v=1$	$J=51-52$	$145\ 190.94 \pm 0.10$	$145\ 190.92$
	$J=63-64$	$178\ 540.49$	$178\ 540.54$
	$J=69-70$	$195\ 180.19$	$195\ 180.16$
$v=2$	$J=51-52$	$144\ 624.81 \pm 0.10$	$144\ 624.75$
	$J=69-70$	$194\ 417.98$	$194\ 418.00$

^a Honig *et al.*, see reference 5. ^b Theoretical estimate.

Cesium Iodide. Cesium iodide is the heaviest diatomic molecule included in the present study, and for this reason its spectra have some interesting features. The spectra were the most difficult for us to interpret. The estimated value of D_e was between 0.13 and 0.18 kc/sec, whereas the value was found to be 0.11 kc/sec, well outside the estimated error calculated by Honig *et al.*⁵ Among the observed CsI lines, a line of slightly greater intensity than most of the others was consistently observed. This anomalous line was finally identified as an H₂O transition at 183 310 Mc/sec, previously observed by King and Gordy.⁷ Apparently H₂O, tightly bound to the CsI molecules, is not released until the CsI is vaporized. In most of the other molecules, the water that sometimes becomes attached to the salt, as in LiBr and LiI, may be released at a lower temperature than that required for vaporization of the salt. Otherwise, it is not known why the water line was not detected during the course of study of the

TABLE XII. Rubidium bromide (Rb⁸⁷Br⁷⁹).

Present results		Previous results	
$Y_{01}^a =$	1409.080 ± 0.015	1409.0573 ± 0.02^b	Mc/sec
$B_0 =$	1406.3406 ± 0.01		Mc/sec
$B_e^a =$	1409.080 ± 0.015		Mc/sec
$\alpha_e = -Y_{11} =$		5.4744 ± 0.0085^b	Mc/sec
$D_e^a = D_0 =$	0.43877 ± 0.0004		kc/sec
Derived constants			
$\omega_e = Y_{10} =$	168.46 ± 0.07		cm^{-1}
$\omega_e x_e = -Y_{20} =$	0.448 ± 0.007		cm^{-1}
$I_e =$	358.766 ± 0.012		$\text{amu } \text{Å}^2$
$r_e =$	2.94471 ± 0.00005		Å
Transitions		Measured lines (Mc/sec)	Calculated lines (Mc/sec)
$v=0$	$J=63-64$	$179\ 551.22 \pm 0.10$	$179\ 551.23$
	$J=64-65$	$182\ 342.01$	$182\ 341.99$
	$J=68-69$	$193\ 498.03$	$193\ 498.03$

Transitions		Measured lines (Mc/sec)	Calculated lines (Mc/sec)
$v=0$	$J=63-64$	$179\ 551.22 \pm 0.10$	$179\ 551.23$
	$J=64-65$	$182\ 342.01$	$182\ 341.99$
	$J=68-69$	$193\ 498.03$	$193\ 498.03$

^a Extrapolated from other constants. ^b Honig *et al.*, see reference 5.

$J=6 \rightarrow 7$ transition of LiI which occurs near this frequency.

Because very high J transitions could be observed, H_e was measured most accurately for CsI. Although H_e is less than 10^{-5} cps for $J=139 \rightarrow 140$, the H_e term makes a contribution of 2.32 Mc/sec to the line frequency. For this heavy molecule, ω_e is only 119 cm^{-1} . Thus, if the pure vibrational transition $v=0-1$ is to be observed with microwave techniques, wavelengths of approximately 0.1 mm must be achieved. In the Duke Microwave Laboratory a wavelength of 0.51 has already been reached with harmonics from an 8-mm klystron.²² With 3-mm klystrons, now available, the pure vibrational spectra of this diatomic molecule may eventually be reached.

²² M. J. Cowan and W. Gordy, Bull. Am. Phys. Soc. 5, 241 (1960).

TABLE XIII. Rubidium iodide (Rb⁸⁶I¹²⁷).

Present results		Previous results	
Y_{01}	984.3066 ± 0.0021	984.3137 ± 0.012^a	Mc/sec
B_e	984.3062 ± 0.0024	984.3166 ± 0.012^a	Mc/sec
$\alpha_e = -Y_{11}$	3.28156 ± 0.0017	3.2806 ± 0.0012^a	Mc/sec
$\gamma_e = Y_{12}$	3.53 ± 0.25	2.98 ± 0.2^a	kc/sec
$D_e = -Y_{02}$	0.221239 ± 0.00011	0.234 ± 0.035^a	kc/sec
$\beta_e = -Y_{12}$	0.000158 ± 0.00008		kc/sec
$H_e = Y_{03} = -17^b$			10^{-6} cps
Present constants		Previous constants	
ω_e	$Y_{10} = 138.511 \pm 0.035$	$147^{a,c}$	cm^{-1}
$\omega_e x_e$	$-Y_{20} = 0.335 \pm 0.006$	0.23^c	cm^{-1}
I_e	513.590 ± 0.018	513.5883^a	$\text{amu } \text{Å}^2$
r_e	3.17684 ± 0.00005	3.1769 ± 0.0001^a	Å
Transitions		Measured lines (Mc/sec)	Calculated lines (Mc/sec)
$v=0$	$J=79-80$	$156\ 773.00 \pm 0.10$	$156\ 773.07$
	$J=98-99$	$193\ 708.04$	$193\ 708.05$
	$J=99-100$	$195\ 647.00$	$195\ 647.05$
$v=1$	$J=79-80$	$156\ 248.91 \pm 0.10$	$156\ 248.83$
	$J=98-99$	$193\ 059.15$	$193\ 059.08$
	$J=99-100$	$194\ 991.56$	$194\ 991.52$
$v=2$	$J=79-80$	$155\ 725.77 \pm 0.10$	$155\ 725.71$
	$J=99-100$	$194\ 337.34$	$194\ 337.38$
$v=3$	$J=79-80$	$155\ 203.66 \pm 0.10$	$155\ 203.73$

^a Honig *et al.*, see reference 5. ^c Barrow and Caunt, see reference 25.
^b Theoretical estimate.

The values obtained for Y_{01} and for B_e in the present study are outside the limit of the estimated error of the data from Honig *et al.*⁵ This might be expected, since an error in Y_{02} of that data would also cause an error in the value of Y_{01} . These spectra were first observed at a temperature of about 630°C. A summary of results for cesium iodide appears in Table XVII.

TABLE XIV. Rubidium iodide (Rb⁸⁷I¹²⁷).

Present results		Previous results	
Y_{01}	970.7523 ± 0.0035	970.7601 ± 0.012^a	Mc/sec
B_e	970.7519 ± 0.0040		Mc/sec
$\alpha_e = -Y_{11}$	3.2133 ± 0.0037	3.2135 ± 0.0030^a	Mc/sec
$\gamma_e = Y_{21}$	3.24 ± 1.2		kc/sec
$D_e = -Y_{02}$	0.21516 ± 0.00015		kc/sec
$\beta_e = -Y_{12}$	0.00015 ± 0.00008^b		kc/sec
$H_e = Y_{03} = -16.4^b$			10^{-6} cps
Derived constants		Previous constants	
ω_e	$Y_{10} = 137.56 \pm 0.05$		cm^{-1}
$\omega_e x_e$	$-Y_{20} = 0.330 \pm 0.006^b$		cm^{-1}
I_e	520.761 ± 0.018		$\text{amu } \text{Å}^2$
r_e	$3.17684 \pm 0.00005 \text{ Å}$		
Transitions		Measured lines (Mc/sec)	Calculated lines (Mc/sec)
$v=0$	$J=80-81$	$156\ 543.86 \pm 0.10$	same
	$J=100-101$	$194\ 879.52$	same
$v=1$	$J=80-81$	$156\ 024.03 \pm 0.10$	same
$v=2$	$J=80-81$	$155\ 505.26 \pm 0.10$	same

^a Honig *et al.*, see reference 5. ^c Extrapolated from other constants.
^b Theoretical estimates.

TABLE XV. Cesium bromide (Cs¹³³Br⁷⁹).

Present results		Previous results	
Y_{01}	1081.33314 ± 0.0020	1081.3392 ± 0.02^a	Mc/sec
B_e	1081.3333 ± 0.0022	1081.3429 ± 0.02^a	Mc/sec
$\alpha_e = -Y_{11}$	3.72052 ± 0.00040	3.7175 ± 0.0029^a	Mc/sec
$\gamma_e = Y_{21}$	3.234 ± 0.044	3.1 ± 0.4^a	kc/sec
$D_e = -Y_{02}$	0.251775 ± 0.000022	0.27 ± 0.08^a	kc/sec
$\beta_e = -Y_{12}$	0.000006 ± 0.000011		kc/sec
$H_e = Y_{03} = -22^b$			10^{-6} cps
Derived constants		Previous constants	
ω_e	$Y_{10} = 149.503 \pm 0.007$	$171^{a,c}$	cm^{-1}
$\omega_e x_e$	$-Y_{20} = 0.3602 \pm 0.0008$	0.3^c	cm^{-1}
I_e	467.506 ± 0.016	467.5039^a	$\text{amu } \text{Å}^2$
r_e	3.07221 ± 0.00005	3.0720 ± 0.0001^a	Å
Transitions		Measured lines (Mc/sec)	Calculated lines (Mc/sec)
$v=0$	$J=53-54$	$116\ 424.56 \pm 0.10$	$116\ 424.57$
	$J=71-72$	$155\ 068.30$	$155\ 068.31$
	$J=72-73$	$157\ 211.47$	$157\ 211.38$
	$J=90-91$	$195\ 705.22$	$195\ 705.28$
$v=1$	$J=53-54$	$116\ 023.35 \pm 0.10$	$116\ 023.45$
	$J=72-73$	$156\ 669.12$	$156\ 669.11$
	$J=91-92$	$197\ 155.57$	$197\ 155.53$
$v=2$	$J=72-73$	$156\ 127.90 \pm 0.10$	$156\ 127.80$
	$J=83-84$	$179\ 507.76$	$179\ 507.80$
$v=3$	$J=73-74$	$157\ 707.97 \pm 0.10$	$157\ 707.80$
	$J=83-84$	$178\ 885.78$	$178\ 885.81$
$v=4$	$J=72-73$	$155\ 048.02$	$155\ 048.00$

^a Honig *et al.*, see reference 5. ^c Barrow and Caunt, see reference 25.
^b Theoretical estimate.

TABLE XVI. Cesium bromide (Cs¹³³Br⁸¹).

Present results		Previous results	
Y_{01}	1064.58192 ± 0.0032	1064.5853 ± 0.02^a	Mc/sec
B_e	1064.5819 ± 0.0042		Mc/sec
$\alpha_e = -Y_{11}$	3.63152 ± 0.0036	3.6313 ± 0.0024^a	Mc/sec
$\gamma_e = Y_{21}$	2.708 ± 0.41	$3.1 \pm 0.5^{a,b}$	kc/sec
$D_e = -Y_{02}$	0.244159 ± 0.00076		kc/sec
$\beta_e = -Y_{12}$	0.000123 ± 0.00046		kc/sec
$H_e = Y_{03} = -22^b$			10^{-6} cps
Derived constants		Previous constants	
ω_e	$Y_{10} = 148.301 \pm 0.023$		cm^{-1}
$\omega_e x_e$	$-Y_{20} = 0.363 \pm 0.035$		cm^{-1}
I_e	474.862 ± 0.023		$\text{amu } \text{Å}^2$
r_e	$3.07221 \pm 0.00005 \text{ Å}$		
Transitions		Measured lines (Mc/sec)	Calculated lines (Mc/sec)
$v=0$	$J=72-73$	$154\ 783.88 \pm 0.10$	$154\ 783.94$
	$J=73-74$	$156\ 893.66$	$156\ 893.64$
	$J=83-84$	$177\ 965.90$	$177\ 965.83$
	$J=91-92$	$194\ 788.37$	$194\ 788.41$
$v=1$	$J=73-74$	$156\ 356.70 \pm 0.10$	$156\ 356.77$
	$J=84-85$	$179\ 453.83$	$179\ 453.70$
	$J=92-93$	$196\ 213.95$	$196\ 214.02$
$v=3$	$J=73-74$	$155\ 285.45 \pm 0.10$	$155\ 285.45$

^a Honig *et al.*, see reference 5. ^b Theoretical estimate.

TABLE XVII. Cesium iodide (Cs¹³³I¹²⁷).

Present results		Previous results	
$Y_{01} = 708.32920 \pm 0.00089$		708.3568 ± 0.02^a	Mc/sec
$B_e = 708.32904 \pm 0.00090$		708.3579 ± 0.02^a	Mc/sec
$\alpha_e = -Y_{11} = 2.04638 \pm 0.00057$		2.0441 ± 0.002^a	Mc/sec
$\gamma_e = Y_{21} = 1.482 \pm 0.082$		1.45 ± 0.4^a	kc/sec
$D_e = -Y_{02} = 0.111330 \pm 0.000025$		0.152 ± 0.025^a	kc/sec
$\beta_e = -Y_{12} = 0.000074 \pm 0.000015$			kc/sec
$H_e = Y_{03} = -7.51^b$			10^{-6} cps
Derived constants		Previous constants	
$\omega_e = Y_{10} = 119.195 \pm 0.013$		$120^{a,c}$	cm ⁻¹
$\omega_e x_e = -Y_{20} = 0.2542 \pm 0.0021$		0.2^c	cm ⁻¹
$I_e = 713.694 \pm 0.025$		713.6686^a	amu Å ²
$r_e = 3.31515 \pm 0.00006$		3.3150 ± 0.0001^a	Å
Transitions	Measured lines (Mc/sec)	Calculated lines (Mc/sec)	
$v=0$	$J=103-104$	$146\ 618.15 \pm 0.10$	$146\ 618.09$
	$J=110-111$	$156\ 412.03$	$156\ 412.02$
	$J=127-128$	$180\ 134.69$	$180\ 134.67$
	$J=134-135$	$189\ 874.72$	$189\ 874.69$
	$J=138-139$	$195\ 432.52$	$195\ 432.49$
$v=1$	$J=110-111$	$155\ 957.84 \pm 0.10$	$155\ 957.98$
	$J=127-128$	$179\ 610.97$	$179\ 610.95$
	$J=128-129$	$180\ 999.32$	$180\ 999.33$
	$J=138-139$	$194\ 863.62$	$194\ 863.63$
$v=2$	$J=110-111$	$155\ 504.71 \pm 0.10$	$155\ 504.61$
	$J=127-128$	$179\ 088.04$	$179\ 087.99$
	$J=138-139$	$194\ 295.66$	$194\ 295.60$
$v=3$	$J=127-128$	$178\ 565.72 \pm 0.10$	$178\ 565.78$
	$J=139-140$	$195\ 104.71$	$195\ 104.71$

^a Honig *et al.*, see reference 5. ^c Barrow and Caunt, see reference 25.
^b Theoretical estimate.

DERIVED RESULTS

Internuclear Distance. The equilibrium value of the fundamental rotational constant B_e can be evaluated with high accuracy from these measurements. From it, the moment of inertia I_e and the equilibrium value r_e of the internuclear distances can be obtained with the relations of Eq. (6). The accuracy of the absolute values of I_e and r_e is limited, however, by Planck's constant h in which the possible error occurs in the fifth significant figure. We have used the value $h = 6.62517 \pm 0.00023$ erg sec given by DuMond and Cohen.²³ The masses employed are those tabulated by Johnson, Quisenberry, and Nier.²⁴ It should be noted that B_e is not measured directly but is calculated from Y_{01} and the other constants which are evaluated from the observed frequencies with Eq. (11). The values for B_e , I_e , and r_e are given in Tables I through XVII.

Vibrational States. In Eq. (3) the first two terms on the right represent the vibrational energy

$$W_v/h = \omega_e(v + \frac{1}{2}) - \omega_e x_e(v + \frac{1}{2})^2. \quad (20)$$

²³ J. W. M. DuMond and E. R. Cohen, in *Handbook of Physics*, edited by E. U. Condon and H. Odishaw, (McGraw-Hill Book Company, Inc., New York, 1958), p. 7.169.

²⁴ W. H. Johnson, K. S. Quisenberry, and A. O. Nier, in *Handbook of Physics*, edited by E. U. Condon and H. Odishaw (McGraw-Hill Book Company, Inc., New York, 1958), p. 9.55.

TABLE XVIII. Bromine isotopes mass ratio.

Molecule	Method	Ratio Br ⁷⁹ /Br ⁸¹	Error
NaBr	Present method	0.9753019	87
RbBr	Present method	0.9753104	66
CsBr	Present method	0.9753132	74
KBr	MBER ^a	0.9753088	20
RbBr	Microwave absorption ^b	0.9752999	65
CsBr	Microwave absorption ^b	0.9753068	45
CsBr	Mass spectroscopy ^c	0.9753075	13

^a Molecular beam electric resonance; see reference 6.

^b See reference 5.

^c See reference 24.

Because $\Delta\nu=0$ in our experiments, we do not obtain the vibrational energies directly but rather by an evaluation of ω_e and $\omega_e x_e$ from the rotational constants with the use of Eqs. (6) and (7). Since the centrifugal stretching constant D_e is evaluated with good accuracy from the high- J millimeter wave transitions (where the stretching effects become large), one can obtain the fundamental vibrational frequency ω_e with good accuracy from Eq. (6c). The much smaller, anharmonic constant $\omega_e x_e$ is also evaluated with better accuracy than previously known. It is of interest that the vibrational structure of these halides is now evaluated indirectly in this way from millimeter wave rotational spectra much more accurately than it could be obtained directly from optical spectroscopy.²⁵ The values obtained for ω_e and $\omega_e x_e$ for the molecules studied are listed in Tables I through XVII along with previous values by others for comparison.

Mass Ratios. For the molecules with atoms having more than one isotope, the mass ratios of any two isotopes (1) and (2) of a given atom can be obtained from the relative B_e values with the relation

$$(B_e^{(2)}/B_e^{(1)}) = (\mu^{(1)}/\mu^{(2)}) \\ = [(M+M_2)/MM_2]/[(M+M_1)/MM_1], \quad (21)$$

from which the mass ratios are

$$M_1/M_2 = (M/M_2)(B_e^{(2)}/B_e^{(1)}) / \\ (1+M/M_2 - B_e^{(2)}/B_e^{(1)}), \quad (22)$$

where $M = M_1 + M_2$. The ratio M/M_2 need not be known precisely for M_1/M_2 to be derived with accuracy. Townes²⁶ shows that a fractional error δ' in M/M_2 gives a fractional error ϵ' in M_1/M_2 of

$$\delta' = (M_2 - M_1)\epsilon' / (M + M_2). \quad (23)$$

Taking account of both the error in $B_e^{(2)}/B_e^{(1)}$ and in M/M_2 , Townes estimates the over-all fractional error in obtaining masses from the B_e ratios of diatomic

²⁵ R. F. Barrow and A. D. Caunt, Proc. Roy. Soc. (London) **A219**, 120 (1953).

²⁶ C. H. Townes and A. L. Schawlow, *Microwave Spectroscopy* (McGraw-Hill Book Company, Inc., New York, 1955), pp. 15-18.

TABLE XIX. Rubidium isotopes mass ratio.

Molecule	Method	Ratio Rb ⁸⁵ /Rb ⁸⁷	Error
RbI	Present method	0.9770162	93
RbCl	MBER ^a	0.9770163	45
RbF	MBER ^a	0.9770148	52
RbI	Microwave absorption ^b	0.9770177	45
RbBr	Microwave absorption ^b	0.9770146	55
RbBr	Mass spectroscopy ^c	0.9770191	22

^a See reference 6. ^c See reference 24.
^b See reference 5.

molecules as

$$\pm \left[\delta \left(\frac{(M/M_2+1)(\mu^{(2)}/\mu^{(1)})}{(M/M_2+1)-\mu^{(1)}/\mu^{(2)}} \right) \pm \Delta \left(\frac{(1-\mu^{(1)}/\mu^{(2)})M_2/M_1}{M/M_2+1-\mu^{(1)}/\mu^{(2)}} \right) \right], \quad (24)$$

where Δ is the fractional error in mass M and δ is the fractional error in $\mu^{(1)}/\mu^{(2)}$.

Tables XVIII and XIX give the mass ratios Br⁷⁹/Br⁸¹ and Rb⁸⁵/Rb⁸⁷ as obtained from the present results. They are believed to be slightly less accurate than the values presently known from other methods. With refinements in the measurements with the present molecular beam spectrometer, these ratios could probably be ascertained to a greater accuracy than the presently known ratios if that were the primary object of these experiments.

Potential Functions. It is interesting to compare the potential constants derived from our data with those from the earlier results of Townes' group⁵ and with those calculated theoretically on the assumption of a completely ionic model by Rittner.²⁷ If Rittner's expression for the bond energy is expanded about the equilibrium point [with $\xi = (r - r_e)/r_e$], it reduces to the form,

$$V = C + A_1 \xi^2 (1 + A_1 \xi + A_2 \xi^2 + \dots) \quad (25)$$

which, except for the constant C , has the form of the dominant term,

$$V = a_0 \xi^2 (1 + a_1 \xi + a_2 \xi^2 + \dots), \quad (26)$$

in Dunham's potential function. Thus, the potential constants a_0 , a_1 , etc. which are derivable from our data are directly comparable to the Rittner constants, A_0 , A_1 , etc. Since the latter are calculated with the assumption of an ionic model, these comparisons give a test of the validity of this model. Such comparisons were previously made by Honig *et al.*,⁵ but our values for the constants a_0 and a_1 of the most significant terms in the Dunham potential should be more reliable than those obtained earlier with less complete data. We

²⁷ E. S. Rittner, J. Chem. Phys. **19**, 1030 (1951).

TABLE XX. Potential coefficients.

Molecule	Previous ^a a_0	Present a_0	Previous ^a a_1	Present a_1	Rittner's ^b A_1
LiBr	1.02	1.42	-2.45	-2.71	-1.71
LiI	1.14	1.35	-2.56	-2.70	-1.75
NaBr	1.64	1.48	-3.16	-3.05	-3.09
NaI	1.74	1.42	-3.23	-3.02	-3.32
KBr	1.63	1.48	-3.35	-3.24	-3.35
KI	1.64	1.43	-3.41	-3.25	-3.50
RbBr	1.73	1.53	-3.49	-3.33	-3.53
RbI	1.64	1.44	-3.49	-3.34	-3.55
CsBr	2.03	1.55	-3.72	-3.38	-4.03
CsI	1.53	1.50	-3.45	-3.43	-3.53

^a See reference 5. ^b See reference 27.

calculate these constants from the more directly derived ones with the Dunham expressions,

$$a_0 = \omega_e^2/4B_e, \quad a_1 = -(\alpha_e \omega_e/6B_e) - 1. \quad (27)$$

Also, a_2 and a_3 can be derived from theoretical expressions involving α_e and γ_e , but our values of a_2 and a_3 are not thought to be more significant than the earlier ones.

Table XX gives a comparison of our values of a_0 and a_1 with those of Honig *et al.* and with the Rittner constant A_1 . The present data show that the a_0 's are much more nearly the same for the different molecules than was indicated by the earlier work. Even the a_0 's for the lithium halides are essentially the same as those for other halides. This uniformity in the a_0 values indicates that the harmonic component in the potential function does not vary much from one alkali halide to another. The peculiarly high value of a_0 for CsBr found in the earlier work is not substantiated.

Our values for a_1 are not the same, within the experimental error, for the different halides but show a small consistent decrease in value from the Cs halides to the Li halides. However, in agreement with the trend earlier found, this decrease is not as much as that of the Rittner A_1 for the completely ionic model. The deviations of our a_1 values from the Rittner A_1 is even wider than that found earlier. This indicates that the com-

TABLE XXI. Comparison of measured $-Y_{11}$ with theoretical Morse α_e .

Molecule	$-Y_{11}$ (Mc/sec)	α_e (Mc/sec)
LiBr ⁷⁹	169.09	162
LiI	122.62	119
NaBr ⁷⁹	28.209	24.4
NaI	19.420	17.9
KBr ⁷⁹	12.136	11.1
KI	8.027	7.40
Rb ⁸⁵ Br ⁷⁹	5.576	5.09
Rb ⁸⁵ I	3.2816	3.07
CsBr ⁷⁹	3.7205	3.38
CsI	2.0464	1.92

pletely ionic model is not valid for the lithium halides, i.e., their bonds have significant covalent character.

As earlier indicated, the Dunham $-Y_{11}$ reduces to the α_e value when the Morse¹⁵ potential,

$$V(r) = V_D [1 - e^{-a(r-r_e)}]^2, \quad (28)$$

is applicable. Table XXI compares the $-Y_{11}$ and α_e values. The comparisons indicate that this compact expression for the potential holds to a good approximation for all the molecules but that it does not provide an exact description for any of them.

Perturbation Energy Coefficients and Ionization Potentials of the Ground State of Three- to Ten-Electron Isoelectronic Atomic Series*

CHARLES W. SCHERR, JEREMIAH N. SILVERMAN,[†] AND F. A. MATSEN
Departments of Physics and Chemistry, The University of Texas, Austin, Texas

(Received January 26, 1962)

The well-known perturbation expansion,

$$E_{nr}^{(N)}(Z) = Z^2 \sum_{i=0}^{\infty} \epsilon_i^{(N)} Z^{-i},$$

of the eigenvalues of the nonrelativistic Schrödinger equation for N electrons about a nucleus of charge Z , has been widely used in the past for the extrapolation and interpolation of atomic energies. The presence of many small effects not explicitly taken into account by the perturbation expansion analysis reduce such calculations to a process of empirical curve fitting of limited range and reliability. These small effects include relativistic effects, the mass polarization, and the Lamb terms; to a good approximation, these effect can also be expanded in a descending power series, but with a leading term containing Z^3 . On the basis of three plausible assumptions, theoretical approximations make it possible, in a semiempirical fashion, to remove a major portion of these small effects from the experimental data. In this way accurate values for $\epsilon_2^{(N)}$ and good estimates for $\epsilon_3^{(N)}$ have been obtained for $3 \leq N \leq 10$. These coefficients have been used to disclose inaccuracies and to fill gaps in the existing atomic energy data and to estimate electron affinities.

I. INTRODUCTION

ELECTRONIC energies of high accuracy for atoms can in theory be obtained by applying the variation principle to a wave function constructed from a large set of suitably chosen basis functions. High accuracy has been obtained only for the He isoelectronic series¹; more recently, such calculations have been made at a somewhat lower level of accuracy for the Li- and Be-isoelectronic series.² Calculations at an equivalent level for a larger number of electrons are not yet available. Further, experimental electronic energies of high accuracy are also not available because, in general, only the first few ionization potentials of a given isoelectronic series have been accurately determined.³ In this paper a semiempirical scheme is developed, based on conventional perturbation theory, for the accurate extrapolation of total electronic energies or of ionization potentials as a function of the nuclear charge. The scheme is used to disclose inaccuracies, to fill gaps in existing experimental data, and to obtain estimates of the electron affinities. The higher-order perturbation energy

coefficients obtained by the analysis are, in themselves of theoretical interest.

For light atoms, the total or experimental energy⁴ $E^{(N)}(Z)$ is given to a good approximation by

$$E^{(N)}(Z) = E_{nr}^{(N)}(Z) + E_r^{(N)}(Z), \quad (1)$$

where Z is the nuclear charge and N is the number of electrons. The $E_{nr}^{(N)}(Z)$ and $E_r^{(N)}(Z)$ are the nonrelativistic and the relativistic energies, respectively, which are defined and discussed separately below.

II. NONRELATIVISTIC ENERGY $E_{nr}^{(N)}(Z)$

The nonrelativistic energy $E_{nr}^{(N)}(Z)$ is the eigenvalue of the appropriate nonrelativistic Schrödinger equation. A well-known result of conventional perturbation theory⁵ is

$$E_{nr}^{(N)}(Z) = Z^2 \sum_{i=0}^{\infty} \epsilon_i^{(N)} Z^{-i}, \quad (2a)$$

where $\epsilon_i^{(N)}$ is the i th-order electronic energy perturba-

* This research was supported in part by the Robert A. Welch Foundation of Houston, Texas.

[†] Present address: National Bureau of Standards, Washington 25, D. C.

¹ C. L. Pekeris, Phys. Rev. **112**, 1649 (1958); **115**, 1216 (1959).

² A. W. Weiss, Phys. Rev. **122**, 1826 (1961).

³ B. Edlén, J. Chem. Phys. **33**, 98 (1960).

⁴ Unless otherwise indicated, the data throughout are in atomic units of energy, $2hcR_M = \mu e^4 \hbar^{-2}$, where R_M is the Rydberg wave number of the atom or ion in question and μ is the appropriate reduced electronic mass.

⁵ See for example, H. A. Bethe and E. E. Salpeter, *Handbuch der Physik*, edited by S. Flügge (Springer-Verlag, Berlin, 1957), Vol. 35, Part 1, p. 214 and p. 237 ff.

FIG. 3. The $J=20 \rightarrow 21$ transition of NaBr^{79} at 187 kMc/sec (1.6-mm wavelength) in the ground vibrational state and in the first and second excited vibrational states. The lines are about 100 kc/sec in width and are distorted by the amplifier because of the rapid sweep used.

